SUPPORTING INFORMATION

Structural basis for distinct functions of the naturally occurring Cys mutants of human apoA-I

Gursky O., Jones M. K., Mei X., Segrest J. P., Atkinson D.

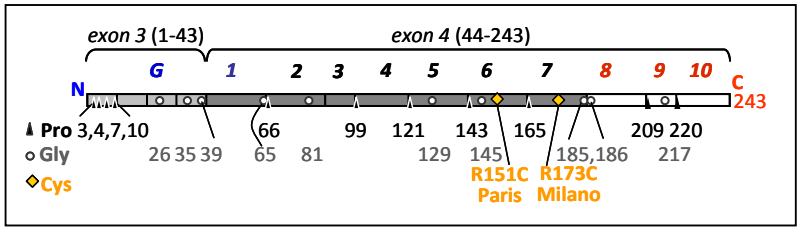

Figure S1. Amino acid sequence repeats in human apoA-I and location of the Milano and Paris mutations. Residues 1-43, encoded by exon 3, form four 10/11-mer G-repeats that have propensity to form class-G amphipathic α-helices similar to those found in globular proteins (1). Residues 44-243, encoded by exon 4, form ten 11/22-mer repeats, marked ***1-10***, that have high propensity to form class-A amphipathic α-helices that form the major lipid surface-binding motif in apolipoproteins (1). C-terminal repeats ***8-10*** are particularly hydrophobic and form the primary lipid binding site in apoA-I. Mutation sites R151C and R173C are located in the middle of helical repeats *6* and *7* in the "left" helical faces (2). This location facilitates formation of intermolecular disulfides in the two antiparallel protein molecules with minimal perturbation of the helical packing in the double belts (2). Positions of Pro and Gly that confer the overall molecular curvature and / or flexibility are indicated.

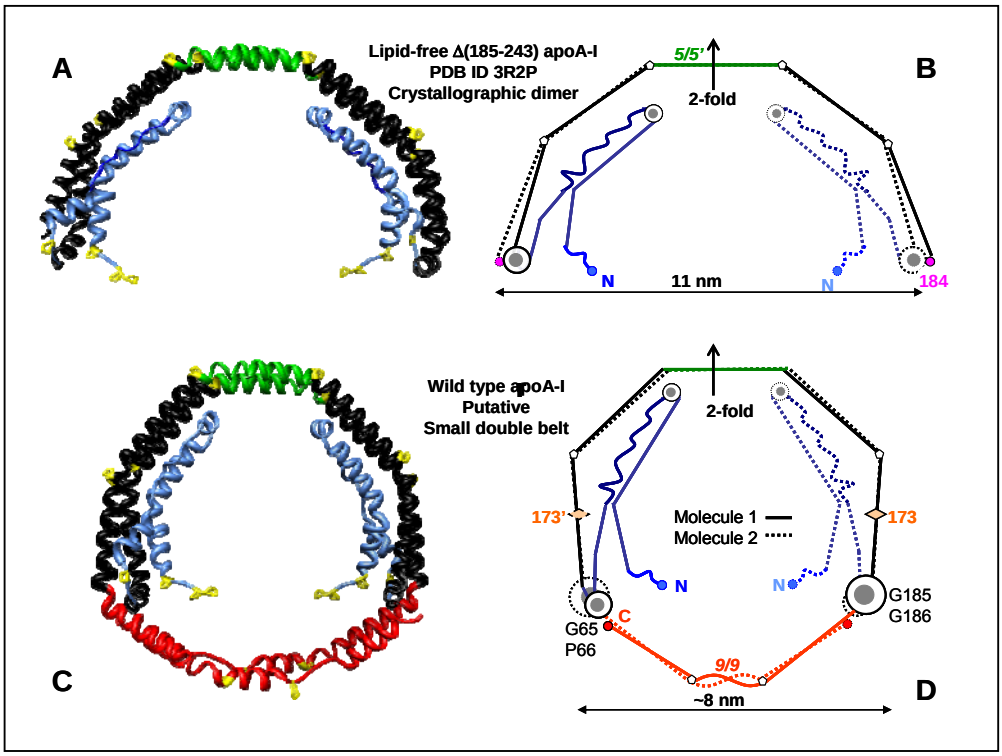

Figure S2. Structure of lipid-free C-terminal-truncated apoA-I solved by Mei and Atkinson (3) (**A, B**) and our structure-based model of the small double belt of full-length wild type apoA-I on HDL (4) (**C, D**). Panels A and C show ribbon representations, and panels B and D show stick structural models. C-terminal residues 185-243 (sequence repeats 8-10) that have been truncated in Δ(185-234)apoA-I are shown in red; their putative conformation resembles that reported in the low-resolution crystal structure of Δ(1-43)apoA-I (PDB ID 1AV1) (5).

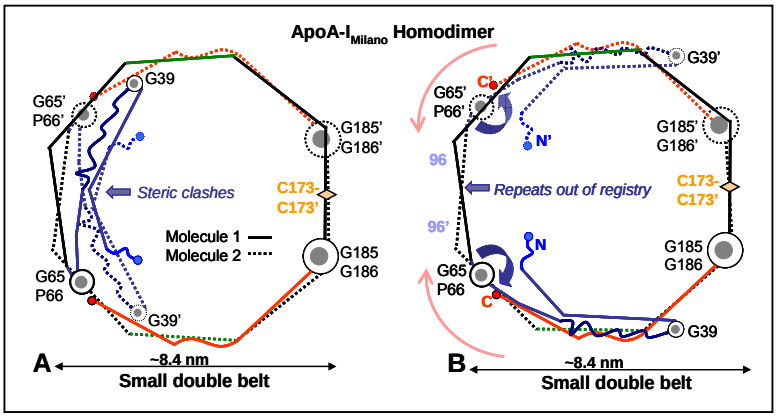

Figure S3. Derivation of the small double-belt conformation of apoA-I$_M$ homodimer on the basis of the previously proposed small double belt of apoA-I$_{WT}$ (4) (shown in Fig. 2B, S2C, D). (**A**) Putative double belt obtained by superimposition of two identical apoA-I conformations. Molecule 1 is shown in the same orientation as in Figure 2C. The antiparallel Molecule 2 is oriented to facilitate intermolecular disulfide link, C173-C173'. The resulting double belt suffers from two apparent drawbacks. First, there are apparent steric clashes between the six overlapping polypeptide segments encompassing sequence repeats ***G-1*** (in blue) and ***2-4*** (in black), whereas only two-to-four such segments can be accommodated on the edge of the phospholipid bilayer in nascent HDL (4). To alleviate these steric clashes, N-terminal segments 1-65 have been rotated away from each other around the G65-P66-containing hinge (**B**, blue circular arrows). The second drawback is lack of helical repeat registry in the parts of the double belt opposite to C173-C173' disulfide (short blue arrow in panels A and B). This can be corrected by constricting the double belt (thin circular arrows, B). The resulting apoA-I$_M$ conformations in a small double belt, in which both these drawbacks have been eliminated, are shown in Fig. 2D (Molecule 1) and Fig. 3A (Molecules 1 and 2 in a symmetric double belt).

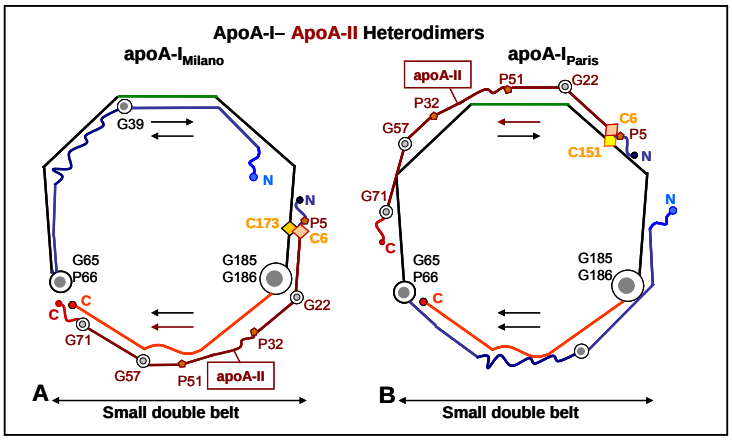

Figure S4. Hypothetical small double belts of apoA-I–apoA-II heterodimers containing Milano and Paris mutations. In these heterodimers, the sole Cys6 in apoA-II forms a disulfide link with the sole Cys173 in apoA-I$_M$ (**A**) or Cys151 in apoA-I$_P$ (**B**). ApoA-II molecule is in brown. Two alternative relative orientations of the apoA-II and apoA-I molecules are depicted in panels A and B. Parallel and antiparallel orientations of the polypeptide chains are shown by arrows. Pro and Gly positions in apoA-I and apoA-II are shown by gray circles. The models were constructed to form closed double belts with maximal Pro kink registry. Similar constraints can be used to derive models of apoA-I–apoA-II heterodimers on larger HDL that contain multiple copies of apoA-I and / or apoA-II (not shown). Since the structures of such apoA-I–apoA-II heterodimers have not been analyzed experimentally (6), these tentative models await their experimental verification.

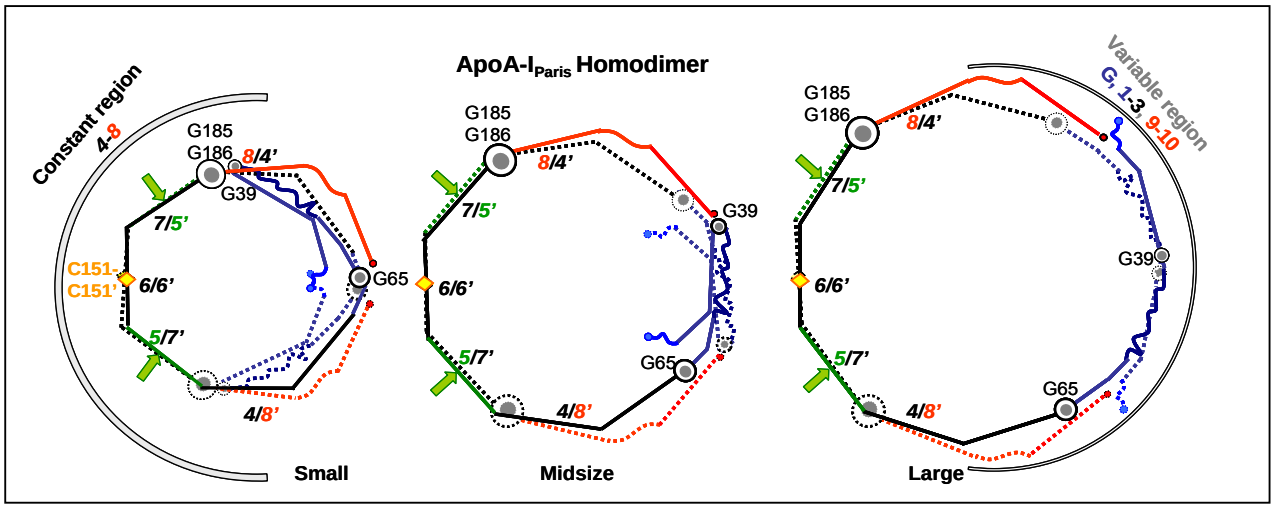

Figure S5. Hypothetical conformational ensemble of apoA-I$_P$ in double belts of various sizes. Intermolecular disulfide C151-C151' that links the two antiparallel molecules of apoA-I$_P$ is shown by a yellow diamond. Constant and variable regions are shown by arcs. Repeat registry in the constant region is indicated. Green arrows point to the center of repeat 5 that forms the lipid presentation tunnel for the LCAT reaction in apoA-I$_{WT}$ on HDL (3). The hinge region G185-G186 in apoA-I$_P$ homodimer is packed against the beginning of repeat 5 at P121 (as opposed to G65-P66 hinge in apoA-I$_{WT}$). Such packing is expected to impair concerted swing motion of the two molecules in the apoA-I$_P$ double belt (Fig. 6, bottom). We propose that this swing motion facilitates tetrafoil conformation of the apoA-I double belt on HDL surface (Fig. 1B). Therefore, we posit that, similar to apoA-I$_M$ (Fig. 6, top panel), apoA-I$_P$ homodimer has impaired ability to adopt a tetrafoil conformation and hence, is expected to form two parallel double belts on spherical HDL (Fig. 1C).

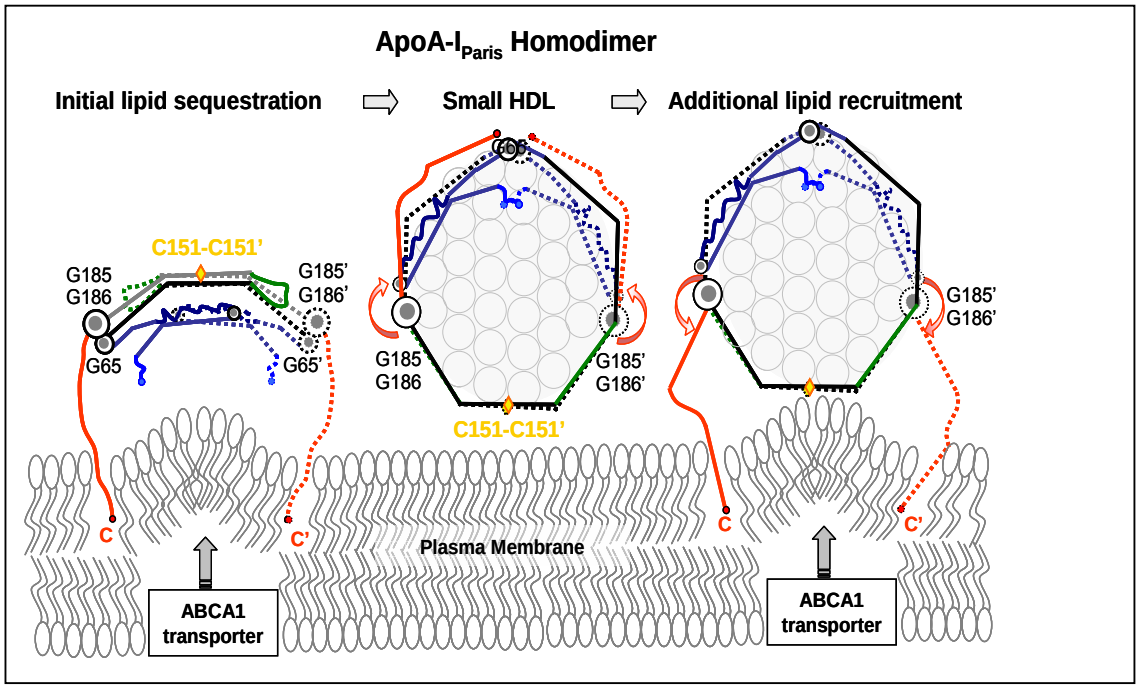

Figure S6. Hypothetical pathway of lipid sequestration by apoA-I$_P$ homodimer and formation of nascent HDL(A-I$_P$–A-I$_P$). We assume that, similar to apoA-I$_M$, apoA-I$_P$ homodimer in solution is comprised of two globular molecules whose conformation resembles that of lipid-free apoA-I$_{WT}$ but, perhaps, is slightly destabilized by mutation. Flexible hinges G185-G186 that confer flexibility to the

C-terminal segments 186-243 (in red) are separated by three 22-mer sequence repeats, *5-7*, in apoA-I_P homodimer (black and green lines between G185-G186 and G185'-G186' at the bottom of the ring). In nascent "discoidal" HDL (shown face up), the protein dimer in a highly helical antiparallel double-belt conformation encircles the phospholipid bilayer; phospholipid head groups in HDL are shown in gray circles. We speculate that, similar to HDL(A-I_M–A-I_M), the C-terminal segments can dissociate from the small HDL(A-I_P–A-I_P) without breaking the double belt (right panel, red circular arrows). We posit that such transient dissociation of the C-terminal segments, which contain the primary lipid binding site in apoA-I, may help recruit additional lipid. This tentative model awaits its experimental verification.

References cited

1. Segrest, J. P., Garber, D. W., Brouillette, C. G., Harvey, S. C., and Anantharamaiah, G. M. 1994. The amphipathic alpha helix: a multifunctional structural motif in plasma apolipoproteins. *Adv. Protein Chem*. 45: 303-369.
2. Brouillette, C. G., Anantharamaiah, G. M., Engler, J. A., and Borhani, D. W. 2001. Structural models of human apolipoprotein A-I: a critical analysis and review. *Biochim. Biophys. Acta* 1531: 4-46.
3. Mei, X., and Atkinson, D. 2011. Crystal structure of C-terminal truncated apolipoprotein A-I reveals the assembly of high density lipoprotein (HDL) by dimerization. *J. Biol. Chem.* 286(44): 38570-38582.
4. Gursky, O. 2013. Crystal structure of Δ(185-243)apoA-I suggests a mechanistic framework for the protein adaptation to the changing lipid load in Good Cholesterol: From Flatland to Sphereland via Double Belt, Belt Buckle, Double Hairpin and Trefoil/Tetrafoil. *J. Mol. Biol.* 425(1): 1-16.
5. Borhani, D. W., Rogers, D. P., Engler, J. A., and Brouillette, C. G. 1997. Crystal structure of truncated human apolipoprotein A-I suggests a lipid-bound conformation. *Proc. Natl. Acad. Sci. USA.* 94: 12291-12296.
6. Rocco, A. G., Mollica, L., Gianazza, E., Calabresi, L., Franceschini, G., Sirtori, C. R., and Eberini, I. 2006. A model structure for the heterodimer apoA-I_{Milano} –apoA-II supports its peculiar susceptibility to proteolysis. *Biophys. J.* 91(8): 3043-3049.